WORLDVIEW-3 SWIR LAND USE-LAND COVER MINERAL CLASSIFICATION: CUPRITE, NEVADA

K.E. Johnson, Staff R&D Scientist
K. Koperski, Principal R&D Scientist
DigitalGlobe, Inc.,
1300 W 120th Avenue,
Westminster, CO 80234
kathleen.johnson@digitalglobe.com
kkopersk@digitalglobe.com

ABSTRACT

Cuprite, Nevada is a location well known for numerous studies of the hydrothermal mineralogy. In particular this region has been used to validate geological interpretations of airborne hyperspectral (AVIRIS HSI), Advanced Spaceborne Thermal Emission and Reflection Radiometer (ASTER) and 8-band satellite SWIR (WorldView-3) imagery. WorldView-3 (WV-3) launched in August 2014, is a high-spatial resolution commercial multispectral satellite sensor with eight visible to near infrared (VNIR) bands (0.42 to 1.04 μm) and eight shortwave infrared (SWIR) bands (1.2 to 2.33 μm). Previous geological studies (Kruse et al., 2015) of WV-3 imagery at Cuprite, Nevada, demonstrated the mineral identification and mapping capabilites of the 8-SWIR bands compared to hyperspectral data (AVIRIS HSI) and ASTER. That study applied Mixture-Tuned-Matched-Filtering (MTMF) analysis. We have applied Land Use-Land Cover (LULC) methods to all 16-bands of data, to perform a geological analysis of WV-3 satellite imagery of the Cuprite, Nevada location. We use the same imagery as the previous WV-3 studies at Cuprite to facilitate the direct comparison of results. The VNIR (1.2 m) and SWIR (7.5m) images were co-registered into a 16-band layer stack for analysis. Ground truth for LULC training and validation was derived from AVIRIS Hyperspectral data and USGS mineral spectral data for this location. We present the results of a supervised LULC classification applying the Random Forest Decision Tree Algorithm with 20 trees. Seven geological materials were tested for identification: Alunite, Calcite, Iron Oxides, Kaolinite, Muscovite, Palagonite (basaltic glass) and Silica (var. chalcedony) with an accuracy of 84% and a kappa coefficient of 0.81 using the DigitalGlobe LULC Web Application. The DG LULC Application includes Gabor Texture, Histogram and Mean values in the analysis. Support Vector Machine Analysis (SPSS-SVM) yields a similar accuracy of 84%. Our experiments show the importance of feature selection for the SVM classifier, while the Tree Classifiers are less sensitive with respect to features. Our results show that with good ground truth, World View-3 SWIR + VNIR imagery produces an accurate geological assessment.

KEYWORDS: WorldView-3, SWIR, Land Use-Land Cover Classification, Cuprite, Mineralogy

INTRODUCTION

WorldView-3 (WV-3), launched in August 2014 by DigitalGlobe, Inc (Westminster, Colorado) is the only 16-band commercial high-resolution Earth imaging satellite currently in orbit. In addition to the 8 visible and near infrared (VNIR: 0.42 to 1.04 μm) bands, WV-3 has the expanded capability of 8 shortwave infrared bands (SWIR: 1.2 to 2.33 μm). The WV-3 SWIR band sensors (Figure 1) were carefully selected to provide remote mineral mapping and materials identification capabilities not available in any other space-borne multispectral system (Kruse et al. 2015). Previous studies by Kruse et al. (2015) and Kruse and Perry (2013) have tested WV-3 SWIR bands only. Both studies applied the Mixture Tuned Matched Filtering (MTMF) method commonly used in AVIRIS classifications. Prior to the launch of WV-3, Kruse and Perry (2013) compared simulated WV-3 data to Cuprite AVIRIS hyperspectral imagery (HSI) and ASTER 6-band 30 m resolution SWIR imagery. Their preliminary findings suggested that WV-3 SWIR bands could be a significant tool for geologic mapping. Following the launch of WV-3, Kruse et al (2015) provided a follow-up study using actual WV-3 SWIR data. This study again compared WV-3 SWIR to AVIRIS HSI, reporting a WV-3 accuracy of 63.23% and Kappa = 0.51, and confirming the predicted mineral identification accuracy of their earlier study.

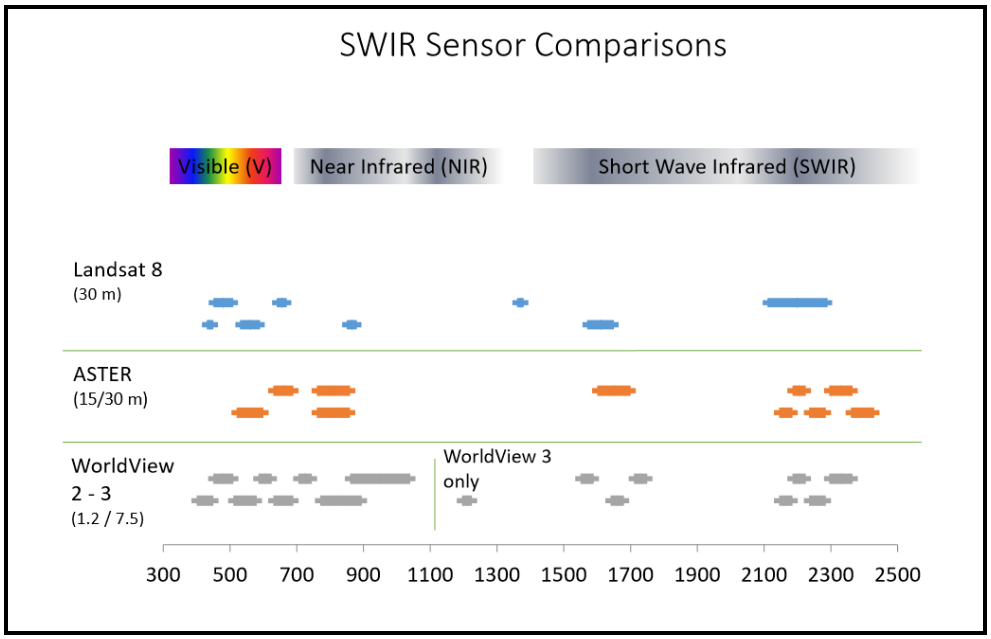

Figure 1. SWIR Sensor Comparison (DigitalGlobe, Inc 2015).

Longbotham et al. (2014) presents a broader simulation study of both unsupervised and supervised classification models for WorldView-3, WorldView-2 and QuickBird. This investigation applied first and second order statistical methods, and mutual information estimates, to the spectral content of the simulated DigitalGlobe sensor data relative to AVIRIS HSI. After the launch of WorldView-3, a preliminary supervised classification analysis applying the same methods to all 16 WV-3 bands for Cuprite, Nevada was undertaken (Longbotham and Johnson 2015). The results of this analysis compared to a more typical LULC scene from San Diego yielded Kappa values of 0.85 for Cuprite, NV and >0.90 for San Diego, CA and comparable urban environments (Longbotham et al. 2015; Longbotham and Johnson 2015).

TABLE 1. MINERALS STUDIED

Mineral	**Description**	**Formula**
Alunite	Hydrous Potassium Sulfate	$(KAl_3(SO_4)_2(OH))_6$
Palagonite	Amorphous weathering product of Basaltic Glass	N/A
Calcite	Calcium Carbonate	$(CaCO_3)$
Iron-Oxides	Goethite Hematite	$(\alpha\text{-}FeOOH)$ (Fe_2O_3)
Kaolinite	Clay Mineral	$(Al_2Si_2O_5(OH)_4)$
Muscovite	Sheet Silicate related to Clays	$(KAl_2(AlSi_3O_{10})(F,OH)_2)$
Silica	var. Chalcedony	(SiO_2)

The goal of this paper is to test the application of DG-LULC classification methods to WV-3 16 band (VNIR + SWIR) imagery for mineral identification. Specifically we describe the DG-LULC method (Marchisio et al. 2015) and we present a DG-LULC classification for key minerals from the Cuprite Mineral District, Nevada (Table 1). As summarized above, WV-3 mineral identification studies focused on the 8 SWIR bands. This paper presents the results of 16-band (VNIR + SWIR) mineral mapping analysis of the Cuprite Mineral District, Nevada, for a low-resolution (SWIR 7.5 m) dataset. Prior experience applying DG-

LULC to WorldView-2 (WV-2) 8-band VNIR imagery suggested that there was also some value in using VNIR bands (Figure 2: bands 6-8) in the classification analysis of geologic materials (Koperski 2012).

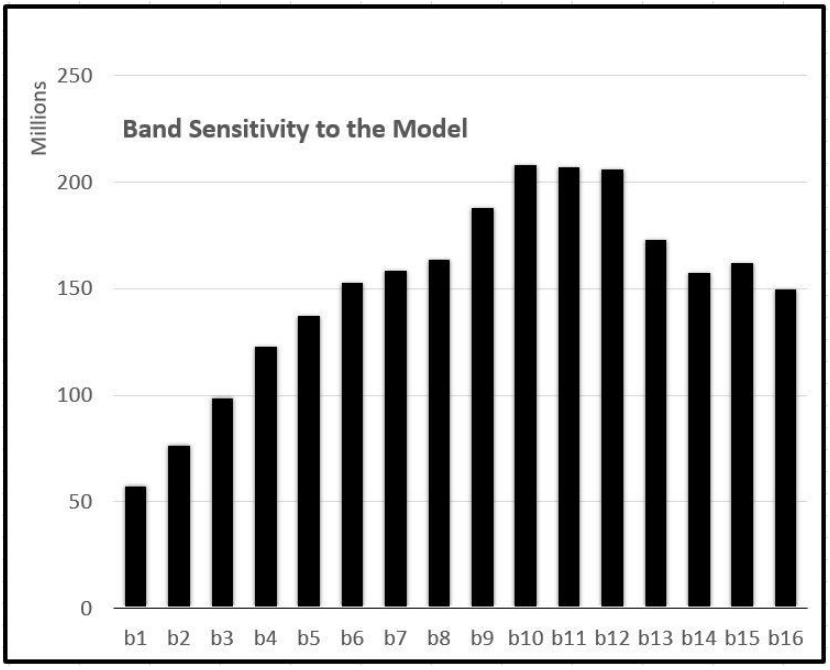

Figure 2. Band sensitivity to the Random Forest Model.

DATA ACQUISITION

We use the WorldView-3 imagery referenced in Kruse et al. (2015). The VNIR and SWIR images were collected simultaneously on September, 19, 2014, at a native resolution of 1.6 m resolution for VNIR and 3.7 m resolution for SWIR. By Law only 7.5 meter SWIR data can be released, so the SWIR data was processed by our automated imagery delivery system, which resamples the SWIR bands to 7.5 m for release. The DG internally developed layer stacking algorithm then resampled the dataset to 1.2 m for both VNIR and SWIR. Therefore, the results published here incorporated the 7.5 m SWIR in the layer stack process. Ground truth was determined from references in Kruse et al. (2015) and Swayze (1997).

SUMMARY OF MODELING TECHNIQUES

DigitalGlobe Land Use-Land Cover Web UI

The DG Land Cover Classification (DG-LULC) method applies the WEKA Open Source JAVA data mining process to image classification (Marchisio et al. 2015). WEKA (Waikato Environment for Knowledge Analysis) accesses a variety of statistical methods for sample analysis through machine learning (Williams 2010; Eibe et al. 2016). For the novice analyst the DG practice is to begin with decision tree methods because they are the robust to outliers generated during the training process (e.g. Biau 2012; Grossmann et al. 2010; Williams 2010; Breiman 2001; Quinlan1986). Decision trees are recursive, i.e. apply the same rule at each node split (Breiman 2001; Quinlan 1986). The decision tree method applied here by DG-LULC is the Random Forest with 20 Trees.

Random Forest employs a bootstrapping method optimized for large datasets with a large number of variables (classes), and is a good starting place for the novice analyst because it: (1) provides a stable model builder with minimal data preprocessing, (2) does not require a normal distribution, (3) is less sensitive to outliers than a single decision tree method and (4) is competitive with nonlinear classifiers such as neural networks.

DG-LULC employs training and validation datasets to initiate each node. Once a tree is completed the next tree is initiated, until all have reached a conclusion. Each node is tested by the percent error of misclassification of the validation dataset (Breiman 2001). The number of decision trees must be specified and can range up to 1000 for very large data sets, with 500 as an average number of trees (Grossmann et al. 2010; Williams 2010). For the very small data sets, as for this study, 20 trees were specified for seven (7) mineral classes. In image classification, the Random Forest method can be subject to bias if care has not been taken to select balanced sample sizes amongst the training classes, and for both training and validation datasets (Grossman et al. 2010). The Random Forest method, e.g., has been applied to Landsat data to generate the USGS GAP Land Cover layers (Grossmann et al. 2010). For the details of the Random Forest method, refer to Breiman (2001).

IBM-SPSS Support Vector Machine (SVM) & C5.0 Analysis

Support Vector Machines (SVM) work by mapping data to a high-dimensional feature space so that data points can be categorized, even when the data are not otherwise linearly separable (IBM SPSS 2017). A separator between the categories is found, the data are then transformed in such a way that the separator could be drawn as a hyperplane. Following this, characteristics of new data can be used to predict the group to which a new record should belong (IBM SPSS 2017). As a classifier, SVM models analyze data and can recognize patterns that distinguish classes for small sample sets (Pandya and Pandya 2015).

C5.0 can produce two types of models: a decision tree or a rule set. In either mode, C5.0 splits the sample based on the fields that provide the maximum normalized information gain (IBM SPSS 2017). As a classifier it can anticipate which attributes are relevant and which are not relevant in the classification (Pandya and Pandya 2015). Large decision trees can be pruned and simplified using rule sets which retain most of the information of the original decision tree (IBM SPSS 2017). Given that our model inputs the data from the DG-LULC Random Forest of 20 trees, only the decision tree mode was applied.

RESULTS AND DISCUSSION

The classification results were assessed by the overall accuracy and the Kappa coefficient (Cohen 1960). The Classification Confusion Matrix is presented in Table 2 and the mineral map produced by the classification is presented in Figure 3. The observed accuracy is based upon running an independent validation dataset against the training dataset. The confusion matrix allows visualization of the algorithm accuracy. Each row represents the instance in the predicted class and each column represents instance in the actual class (Viera et al. 2005). The results for this classification has an observed accuracy of 84.3% with a kappa coefficient of 0.809 (Table 2). The Kappa coefficient is a measure of precision which takes into account the case where two independent observers (e.g. the training and validation datasets) may agree or disagree simply by chance (Viera et al. 2005). A Kappa = 1 represents perfect agreement between the observers, and a Kappa = 0 represents agreement simply by chance.

TABLE 2. DG-LULC Confusion Matrix: Random Forest 20 Trees

Accuracy % Observed Accuracy: 0.843 Kappa coefficient: 0.809

Classes	Alunite	Fe-oxides	Kaolinite	Palagonite	Muscovite	Calcite	Silica	Accuracy
Alunite	57.88	0.09	0.50	0.39	32.98	8.16	0.00	57.88
Iron_oxides	27.38	65.27	5.28	0.02	1.99	0.05	0.02	65.27
Kaolinite	1.21	0.46	95.41	0.00	0.00	0.00	2.91	95.41
Palagonite	5.17	0.71	0.00	91.20	0.42	2.50	0.00	91.20
Muscovite	6.18	0.00	0.00	0.00	92.64	1.17	0.00	92.64
Calcite	0.05	0.00	4.84	0.00	19.53	74.52	1.06	74.52
Silica	0.00	0.00	13.23	0.00	0.00	0.00	87.77	86.77
TOTAL	5164	2955	11655	5664	16500	8121	3325	100.00

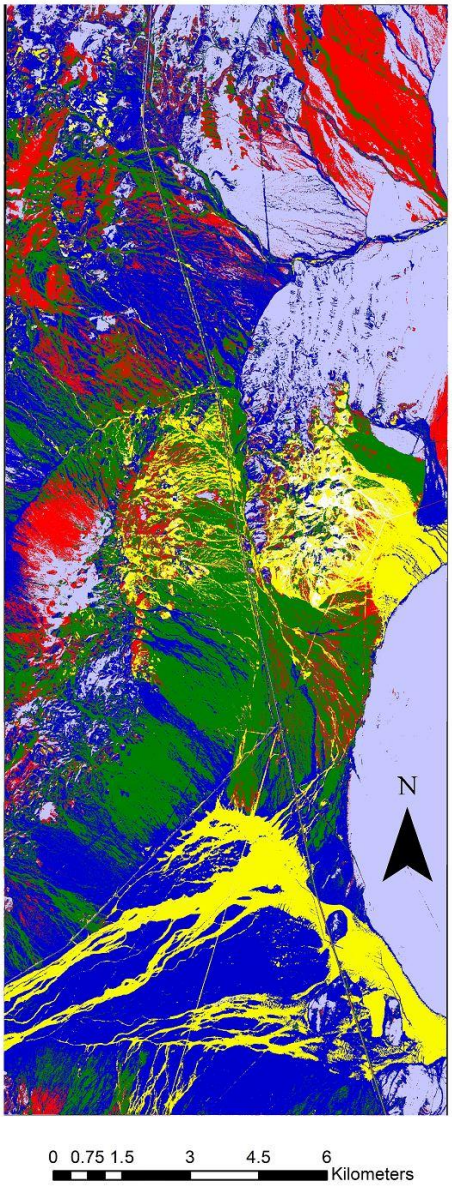

Figure 3a

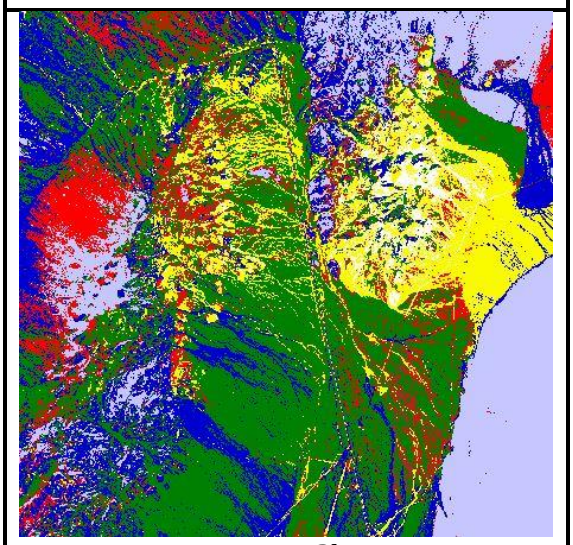

Figure 3b

Figure 3. Classification results for this study produce by the DG –LULC algorithm. Figure 3a shows the entire area of interest classified; 3b shows a zoom of the region discussed by Kruse et al. (2015).

The results of testing several classifiers and various parameter combinations are presented in Table 3. The model parameters and data imported from DG-LULC are: 8-band VNIR, 8-band SWIR, separate VNIR and SWIR normalized band ratios, Gabor Texture, Histogram, Mean. The DG-LULC results compare favorable to both SVM Random Forest and WEKA Random Forest models that have applied all of the parameters.

Classifiers can be boosted to potentially improve the predictive performance. Boosting works by successive reweighting the training dataset based on the classifier's previous performance. Boosting is most successful when applied to unstable classifiers, such as decision trees. In this case, boosting was applied to the C5.0 classifier. Although the VNIR bands 6-8 do contribute significantly to the classification results, the accuracy of the VNIR-only results are significantly decreased. This reinforces the importance of the SWIR bands to the overall classification results and the VNIR-only accuracies fall outside the accepted range for DG-LULC accuracy (Koperski 2012).

Table 3. Model Accuracy Comparison (%)					
DG LULC Model* VNIR + SWIR, Random Forest 20 Trees: 84.3%, Kappa Coefficient = 0.809					
MODEL Comparisons	**SVM[1]**	**C5.0[2] 20 Boosted Trees**	**WEKA[3] Random Forest 20 Trees**	**WEKA[3] Random Forest 40 Trees**	**WEKA[3] Random Forest 100 Trees**
All LULC Features Included*	76.58	79.80	82.55	83.26	82.83
VNIR, SWIR, Mean and Histogram	76.67	79.91	80.73	81.18	82.2
VNIR, SWIR and Mean	84.00	81.44	82.20	83.28	84.69
VNIR and SWIR	83.73	82.92	80.54	82.79	83.68
VNIR Only	61.64	64.43	64.14	64.54	64.67
SWIR Only	76.98	74.55	75.30	76.08	76.86
*LULC Parameters as defined by the DG LULC Model: 8-band VNIR, 28 VNIR Normalized Band Ratios, 8-band SWIR, 28 SWIR Normalized Band Ratios, Gabor Texture, Histogram, 16 Spectral 3x3 Mean Values. 1-IBM SPSS Support Vector Machine Model 2-IBM SPSS C5.0 Model 3-WEKA Machine Learning Suite (http://www.cs.waikato.ac.nz/ml/index.html)					

CONCLUSIONS

We have demonstrated through predictive statistical analysis that VNIR bands 6-8 (Red Edge, NIR1, NIR2) do contain valuable information, and are comparable in sensitivity to some of the SWIR bands, such as bands 14-16 (Figure 2). Our overall findings show that DG-LULC classification analysis using all 16 WV-3 bands provides a quick and accurate solution for mineral/geologic mapping. As with any supervised classification method, accuracy of mineralogical classification depends on high quality ground truth.

REFERENCES

Biau G, 2012. Analysis of a random forest model, *Journal of Machine Learning*, 13:1063-1095.

Breiman L., 2001. Random Forests, *Machine Learning*, 45:5-32.

Cohen J, 1960. A coefficient of agreement for nominal scales. *Educational and Psychological Measurement*, 20:37-46.

DigitalGlobe Inc., "Worldview-3 specifications", 2015. https://www.digitalglobe.com/sites/default/ files/DG_WorldView3_DS_forWeb_0.pdf

Eibe Frank, Mark A. Hall, and Ian H. Witten, 2016. *The WEKA Workbench. Online Appendix for: Data Mining: Practical Machine Learning Tools and Techniques*, Morgan Kaufmann, Fourth Edition, 2016.

Grossmann E. J. Ohmann, J. Kagan, H. May and M. Gregory, 2010. Mapping ecological systems with a Random Forest model: Trade-offs between errors and bias, *Gap Analysis Bulletin*, 17:16-22.

IBM SPSS Modeler [Version 15.0], 2017. IBM Knowledge Center, https://www.ibm.com/support/knowledgecenter/

Koperski K., 2012. IARPA Finder Project Phase I, unpublished report to IARPA, https://www.iarpa.gov/index.php/research-programs/finder/

Kruse F.A. and S.L. Perry, 2012. Mineral mapping using simulated short-wave-infrared bands planned for

DigitalGlobe WorldView-3, in Proc. *Imaging and Applied Optics Technical Digest*, Monterey, California, Paper RM3E.4.pdf (CD-ROM), Optical Society of America, Washington, D. C.

Kruse F.A., W.M. Baugh and S.L. Perry, 2015. Validation of DigitalGlobe WorldView-3 Earth imaging satellite shortwave infrared bands for mineral mapping. *Journal of Applied Remote Sensing*, 9: 1-17.

Longbotham N. and K.E. Johnson, 2015. Unpublished data.

Longbotham N., F. Pacifici, S. Malitz, W. Baugh, G. Camps-Valls, 2015. Measuring the Spatial and Spectral Performance of WorldView-3, in *Hyperspectral Imaging and Sounding of the Environment* (HISE), 2015.

Longbotham N., F. Pacifici, W.M. Baugh and G. Camps-Valis 2014. Prelaunch assessment of WorldView-3 information content, *Workshop on Hyperstectral Image and Signal Processing: Evolution in Remote Sensing*, WHISPERS, Lausanne, Switzerland, https://www.researchgate.net/publication/283876097

Marchisio G.B., C. Tusk, K. Koperski, M.D. Tabb and J.D. Shafer, 2015. Classification of land based on analysis of remotely-sensed earth images, DigitalGlobe, Inc: US Patent #9147132 B2

Pandya R. and J. Pandya, 2015. C5.0 algorithm to improved decision tree with feature selection and reduced error pruning. *International Journal of Computer Applications*, 117: 18-21.

Quinlan J.R., 1986. Induction of decision trees, *Machine Learning*, 1:81-106.

Swayze G.A., 1997. The hydrothermal and structural history of the Cuprite Mining District, southwestern Nevada: an integrated geological and geophysical approach, unpublished Ph.D. Dissertation, Univ. of Colorado at Boulder, pp. 399, Boulder, Colorado.

Williams G., 2010. *Data mining desktop survival guide*, https://www.togaware.com/datamining/survivor/